

Spatiotemporal characteristics of the time of emergence for anthropogenic tropospheric temperature changes based on the CMIP6 multi-model results

Article

Published Version

Creative Commons: Attribution 4.0 (CC-BY)

Open Access

Zhang, S., Liu, X. and Dong, B. ORCID: <https://orcid.org/0000-0003-0809-7911> (2024) Spatiotemporal characteristics of the time of emergence for anthropogenic tropospheric temperature changes based on the CMIP6 multi-model results. *Environmental Research Letters*, 19 (4). 044052. ISSN 1748-9326 doi: <https://doi.org/10.1088/1748-9326/ad34e6> Available at <https://centaur.reading.ac.uk/115859/>

It is advisable to refer to the publisher's version if you intend to cite from the work. See [Guidance on citing](#).

To link to this article DOI: <http://dx.doi.org/10.1088/1748-9326/ad34e6>

Publisher: Institute of Physics

All outputs in CentAUR are protected by Intellectual Property Rights law, including copyright law. Copyright and IPR is retained by the creators or other copyright holders. Terms and conditions for use of this material are defined in the [End User Agreement](#).

www.reading.ac.uk/centaur

CentAUR

Central Archive at the University of Reading

Reading's research outputs online

LETTER • **OPEN ACCESS**

Spatiotemporal characteristics of the time of emergence for anthropogenic tropospheric temperature changes based on the CMIP6 multi-model results

To cite this article: Shulei Zhang *et al* 2024 *Environ. Res. Lett.* **19** 044052

View the [article online](#) for updates and enhancements.

You may also like

- [When will trends in European mean and heavy daily precipitation emerge?](#)
Douglas Maraun
- [Even mild respiratory distress alters tissue oxygenation significantly in preterm infants during neonatal transition](#)
Bernhard Schwabegger, Gerhard Pichler, Corinna Binder *et al.*
- [Automatic Adjustments of a Trans-oesophageal Ultrasound Robot for Monitoring Intra-operative Catheters](#)
Shuangyi Wang, James Housden, Davinder Singh *et al.*

The Breath Biopsy® Guide
Fourth edition

FREE

DOWNLOAD THE FREE E-BOOK

BREATH BIOPSY

OWLSTONE MEDICAL

ENVIRONMENTAL RESEARCH
LETTERS

LETTER

OPEN ACCESS

RECEIVED
4 December 2023REVISED
22 February 2024ACCEPTED FOR PUBLICATION
18 March 2024PUBLISHED
28 March 2024

Original content from
this work may be used
under the terms of the
[Creative Commons
Attribution 4.0 licence](#).

Any further distribution
of this work must
maintain attribution to
the author(s) and the title
of the work, journal
citation and DOI.

Spatiotemporal characteristics of the time of emergence for
anthropogenic tropospheric temperature changes based on the
CMIP6 multi-model resultsShulei Zhang^{1,2,*}, Xiaodong Liu^{1,2,*} and Buwen Dong³ ¹ State Key Laboratory of Loess and Quaternary Geology, Institute of Earth Environment, Chinese Academy of Sciences, Xi'an, People's Republic of China² University of Chinese Academy of Sciences, Beijing, People's Republic of China³ National Centre for Atmospheric Science, Department of Meteorology, University of Reading, Reading, United Kingdom

* Authors to whom any correspondence should be addressed.

E-mail: zhangshulei@ieecas.cn and liuxd@loess.llqg.ac.cn**Keywords:** tropospheric temperatures, surface air temperature, anthropogenic activities, internal climate variability, time of emergence (TOE), CMIP6Supplementary material for this article is available [online](#)**Abstract**

In the 20th century, with the intensification of human activities, the Earth is experiencing unprecedented warming. However, there are certain differences in the sensitivity of temperature changes to anthropogenic forcings in different regions and at different altitudes of the troposphere. The time of emergence (TOE) is the key point at which the anthropogenic climate change signal exceeds from the internal climate variability serving as a noise. It is a crucial variable for climate change detection, climate prediction and risk assessment. Here, we systematically analyzed the spatiotemporal characteristics of the TOE of temperature changes over the past century by calculating the SNR based on the selected CMIP6 multi-model outputs. The results show that the temperature TOE, particularly in the lower and middle troposphere, shows distinct latitude dependence, displaying an 'M-type' distribution from the Antarctic to the Arctic: it first appears in low-latitudes, followed by high-latitudes, and last appears in the two mid latitude bands. For the tropics, the TOE of tropospheric temperatures becomes earlier with increasing altitude: the TOE of air temperatures at the surface, mid-tropospheric 500 hPa and upper-tropospheric 200 hPa occurs in 1980 ± 15 , 1965 ± 20 , and 1930 ± 30 , respectively. The TOEs of tropospheric temperatures in eastern equatorial Pacific are 10–30 years later than those in the western equatorial Pacific. For the regional TOEs of surface air temperature diverse differences exist on land and ocean in various latitudes of two hemispheres.

1. Introduction

Since the industrial revolution, the atmospheric concentration of CO₂ has risen rapidly, exceeding 410 ppm today, the highest level in the past 2 million years (Connors *et al* 2022). Earlier climate modeling study (Manabe and Wetheral 1967) suggested that doubling CO₂ level could cause a 2 °C–3 °C increase in atmospheric temperature. Currently, the global mean surface temperature has already risen by more than 1 °C relative to the pre-industrial period (Allen *et al* 2018). Previous studies attributed the

global warming over the past century mainly to the increasing anthropogenic greenhouse gas emissions (Bindoff *et al* 2013, Haustein *et al* 2017, Gillett *et al* 2021). The latest IPCC Assessment Report (Eyring *et al* 2021) confirmed.

While most regions globally have presented an overall warming trend throughout the 20th century (Jones *et al* 1999, Solomon *et al* 2007), the contemporary climate warming trend varies spatially. Higher latitudes generally experienced more significant surface temperature increases than lower latitudes (England *et al* 2021, Rantanen *et al* 2022), with

land warming surpassing ocean warming (Karoly and Wu 2005, Joshi *et al* 2008, Dong *et al* 2009). High-elevation regions like the Tibetan Plateau exhibited more pronounced warming than low-elevation areas at the same latitudes (Liu and Chen 2000, Pepin *et al* 2015). Regarding variations of atmospheric temperature in the whole troposphere, satellite observations indicated that temperature changes at the upper troposphere in the tropics exceeded those at the surface (Fu *et al* 2004, Santer *et al* 2005). More generally, the warming trend in the troposphere intensified with altitude in the tropics, with greater warming observed at higher altitudes than at the surface (Fu *et al* 2011, Mitchell *et al* 2013). Numerous modeling results from early atmospheric global circulation models (Manabe and Wetherald 1975) and state-of-the-art coupled atmosphere-ocean climate models (Vallis *et al* 2015, Santer *et al* 2017) consistently indicated that the warming in the tropical upper troposphere surpassed that in the lower troposphere, with the maximum warming occurring at approximately 200 hPa.

The global mean temperature change over the past century displayed non-monotonic warming, with notable multi-decadal fluctuations (Kosaka and Xie 2016, Dong and McPhaden 2017). Previous studies (Tett *et al* 1999, Stott *et al* 2000, Medhaug *et al* 2017) revealed that external forcings, including anthropogenic forcings and natural forcings contributed to the long-term trend in global mean surface temperature over the 20th century. Additionally, interdecadal variations in surface temperature were influenced by internal climate variability (such as the Interdecadal Pacific Oscillation, IPO, e.g. England *et al* 2014, Dai *et al* 2015, Meehl *et al* 2016 and the Atlantic Multidecadal Oscillation, AMO, e.g. Steinman *et al* 2015, Chen and Tung 2018, Wei *et al* 2019). At the multi-decadal scale, the internal climate variability and anthropogenic forcing are two major factors affecting climate change (Hulme *et al* 1999, Deser *et al* 2012a). By quantifying the signal-to-noise ratio (SNR) of the 'signal' (climate changes induced by the anthropogenic radiative forcing) relative to the 'noise' (internal climate variability), the time of emergence (TOE) method is increasingly being used to detect anthropogenic climate changes regionally (Hawkins and Sutton 2012). The TOE can not only clarify when climate change occurred in different regions in the past and identify regions affected by anthropogenic global warming, but it can also predict the timing of future climate change. It serves as a key indicator for conducting risk assessments and proposing adaptation strategies for future climate projections (Estrada *et al* 2021).

The TOE for various climate variables has been extensively studied over the past, including global annual mean air temperature (Chen *et al* 2021,

Im *et al* 2021), seasonal mean air temperature (Mahlstein *et al* 2011, 2012, Deser *et al* 2016, Lehner *et al* 2017), annual mean precipitation (Zhang and Delworth 2018), seasonal mean precipitation (Chen *et al* 2021), GHGs-forced precipitation change hot-spots (PSPOTs) (Giorgi and Bi 2009), and extreme climate indices (Fischer and Knutti 2014, King *et al* 2015). Surface temperature TOE patterns are inconsistent with warming patterns (Mahlstein *et al* 2012), in certain latitudes with the smaller (larger) signal probably exhibiting the earlier (later) TOE. However, several results are still somewhat different (Hawkins and Sutton 2012, King *et al* 2015, Chen *et al* 2021) due to the variations in signal and noise calculation methodologies, thresholds of SNR, and emission scenarios. The estimation of TOE is also subject to model parameterizations, statistical tests for the robustness, and the uncertainties of internal climate variability (Tebaldi and Knutti 2007, Hawkins and Sutton 2009, Deser *et al* 2012b, Lehner *et al* 2017). On the other hand, Santer *et al* (2019) examined the detection times in temperatures in the lower stratosphere and the troposphere for the globe, Northern Hemisphere (NH) and Southern Hemisphere (SH), suggesting that the global detection time in the lower stratosphere is earlier than troposphere. Whether TOE patterns for tropospheric temperature at different altitudes are consistent with global warming remains unknown, and few research has systematically analyzed the temporal and spatial differences in the TOE of air temperatures. In this study, we assess the spatial and temporal variations in the annual mean temperature TOE using multivariate statistical methods and to evaluate physical processes for these variations based on selected CMIP6 model outputs.

2. Data and methods

For simulated temperatures, we utilized monthly mean sea surface, surface air, 500 hPa and 200 hPa temperatures stem from the ensemble member (r1i1p1f1) of pre-industrial (piControl, ≥ 500 years) and historical (1850–2014) experiments by 11 atmosphere-ocean general circulation models (AOGCMs) (table S1 in supplementary information part I) in CMIP6 (Eyring *et al* 2016). For observed temperatures, two monthly mean temperatures were used: (1) SSTs in National Oceanic and Atmospheric Administration Extended Reconstruction Sea Surface air temperatures Version 5 (ERSSTv5, $2^\circ \times 2^\circ$, 1854–2014, Huang *et al* 2017). (2) Tropospheric temperatures, including surface, 500 hPa, and 200 hPa temperatures in the fifth generation ECMWF atmospheric reanalysis of the global climate (ERA5, $0.25^\circ \times 0.25^\circ$, 1959–2014, Hersbach *et al* 2020). All model outputs as well as observed data were bilinearly interpolated into $1^\circ \times 1^\circ$ resolution. Additionally, all monthly

means were converted to annual means, calculated from January to December.

The Taylor Skill (TS) Score, which served as a metric for comprehensive evaluation of climate model simulation performance (Taylor 2001, Wang *et al* 2018), was used in this study to determine the extent to which simulations closely approximate actual observations (supplementary information part II). Based on the TS scores of 11 AOGCMs, 8 models were selected for the following multi-model ensemble mean (MEM) analysis. More information for model selection is provided in supplementary information part I.

Consistent with Hawkins and Sutton (2012), we initially calculated the SNR by estimating the signal and noise for temperatures and then identified the TOE for grid. To obtain the signal of annual mean temperature at a specific model grid point, we fitted the global annual mean temperature change sequence to a fourth order polynomial $G(t)$ (t , time) to capture the long-term trend, and finally obtained the signal $S(x,y,t)$ for each model. The annual mean temperature change (1850–2014) at grid point (x,y) is relative to the mean during the reference period (1850–1899), which served as a proxy for pre-industrial period.

$$S(x,y,t) = \alpha(x,y) \cdot G(t) + \beta(x,y).$$

Here, α represents the regression coefficient, indicating the response of the annual mean temperature at grid point (x,y) to global warming, and β is the intercept. The noise, i.e. the standard deviation of the annual mean temperature at each grid, using the piControl simulations (Stocker *et al* 2014). Finally, the first year in which the grid signal consistently exceeds the noise was identified as the TOE. The MEM TOE was calculated based on MEM signal and noise. The observed grid-point SST signal is relative to 1854–1899 mean and noise is derived by subtracting grid point SST series from signals. We used the bootstrap percentile method to evaluate the robustness of MEM TOE (supplementary information part III).

3. Results

3.1. TOE of tropical sea surface temperature

To demonstrate the simulating ability of MEM TOE, its comparison with the observation is essential. The MEMs of annual mean SST signal, noise, SNR and TOE spatial patterns respectively resemble those in observations. Both show pronounced warming signals (figures 1(a) and (b)) but relatively higher noise in the eastern equatorial Pacific (figures 1(c) and (d)). Thus, the corresponding TOE is delayed (emerging after 2000) in comparison with other tropical regions where TOE occurs around the 1970s or 1980s

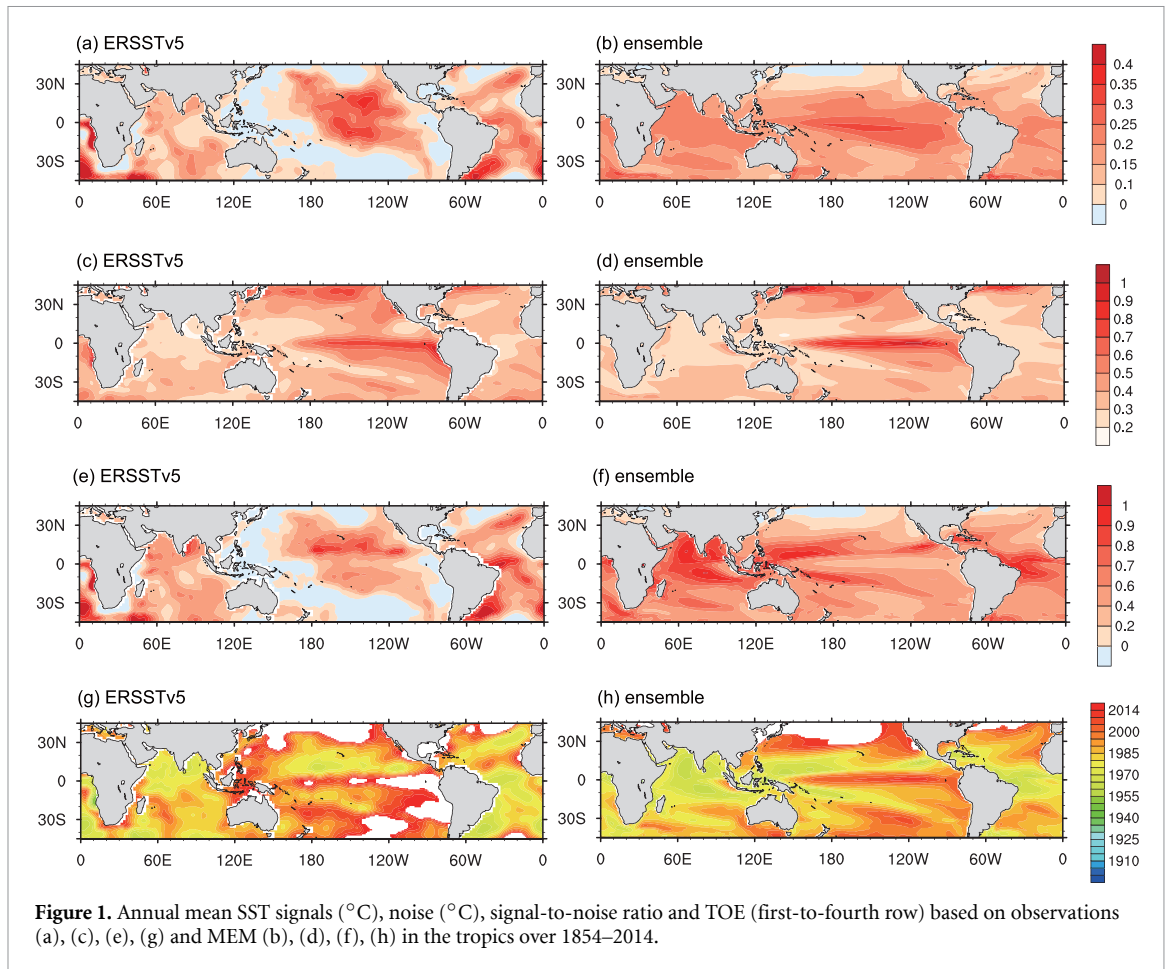
(figures 1(g) and (h)). These regional differences indicate that the magnitude of noise significantly affects the TOE. Furthermore, the SNR (figures 1(e) and (f)) is in good agreement with TOE spatially, with regions exhibiting a larger SNR showing earlier TOE.

3.2. TOEs of tropospheric temperatures

Given the consistence between MEM and observation TOEs of tropical SSTs, we further investigated the MEM signal, noise, and TOE of tropospheric temperatures. The signal patterns at different levels mirror the corresponding warming trends. The signal varies distinctly across different altitudes. For surface air temperature, land shows a more pronounced warming signal than ocean at the same latitudes, particularly in the NH high latitudes where the changes are more intense (figure 2(f)). Low-to-mid latitudes of the SH have larger signals in the mid-tropospheric 500 hPa temperature (figure 2(e)). The upper-tropospheric 200 hPa temperature displays the most noticeable warming trend in the tropics and a cooling trend in the SH high latitudes (figure 2(a)). The noise (figures 2(g)–(i)) exhibits a certain degree of polar amplification, indicating significantly higher internal climate variability in mid-to-high latitudes than that in the tropics.

Consistent with SST SNR and TOE pattern, large SNRs for temperatures in the tropics always result in early TOE. For surface air temperature, the strong noise level (figure 2(i)) in the NH high-latitudes results in a delayed TOE (emerging after 1970) compared to the tropics (figure 2(o)). Conversely, despite the tropics displaying relatively smaller warming signals (figure 2(f)), they experience greater temperature changes relative to interannual noise compared to other regions, resulting an earlier TOE, commencing around 1940. The comparatively lower warming signals and higher interannual noise lead later TOEs in the mid-latitudes. Our observational analysis (supplementary information part IV) reveals earlier TOE in the tropics, aligning with Mahlstein *et al* (2012). However, the observational TOE in high-latitudes is later than that in the simulations. This discrepancy may be attributed to the sparser and possibly less accurate observational records in high-latitudes, necessitating further research.

Due to various reasons, previous studies showed some differences and similarities in the obtained surface air temperature TOE with this study. For example, there is a 40–60 year lag in the global temperature TOE from Hawkins and Sutton (2012) compared to our result, highlighting the impact of different baseline periods and emission scenarios. King *et al* (2015) applied the Kolmogorov–Smirnov (KS-) test revealed that the earliest TOE in tropical Africa



and Indonesia emerged in the 1940s, which is consistent with ours. However, the different reference period in the KS-test (Mahlstein *et al* 2012) may lead different first emergences in the tropics. Chen *et al* (2021) distinguished anthropogenic climate change from internal climate variability and found that the TOE in tropics emerged around 1970s, which is later than ours. Christensen *et al* (2007) defined the change (internal variability) in 20 year means of annual mean temperature as the signal (noise). Despite the various calculations, the latitudinal distribution of TOE generally remains consistent with our results.

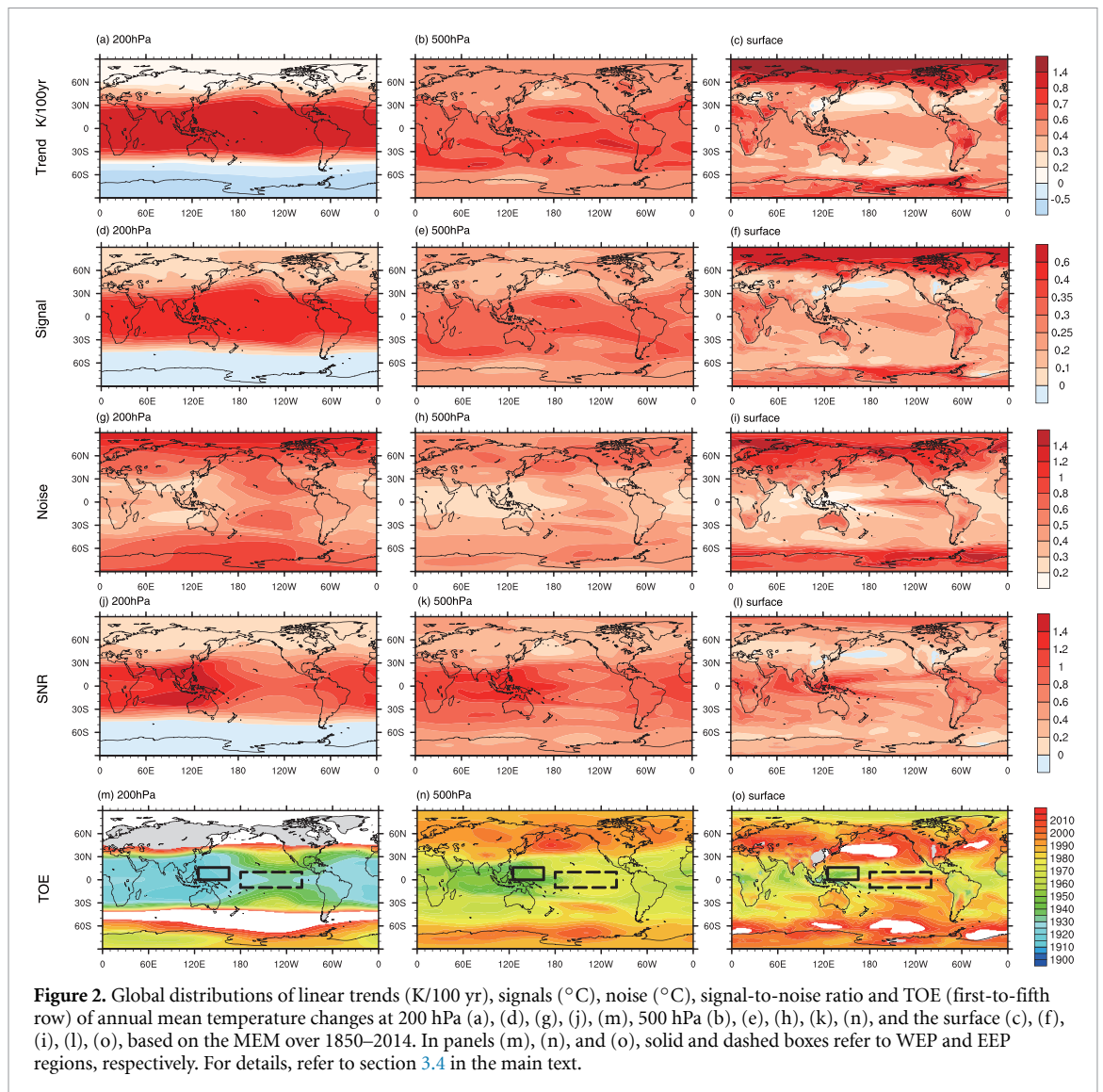
Our analysis (figures 2(m)–(o)) reveals TOE differences exist in different levels based on the SNR by Hansen *et al* (1988). We highlight lower and mid tropospheric 500 hPa temperature TOE in the tropics (around 1960s–1980s) occurs 30–50 years later than that in the upper tropospheric 200 hPa (around 1930s). The tropics exhibit more notable warming signals in the upper troposphere (figures 2(d)–(f)), which may be responsible for TOE variations with altitudes over the tropics in the troposphere.

The warming signals are largely driven by surface warming patterns, which is also related to the water vapor and lapse rate feedback (Soden and

Held 2006, Po-Chedley *et al* 2018). In the tropics, the vertical temperature profile is predominantly determined by radiative-convective equilibrium. External forcings-induced surface temperature increasing leads to higher water vapor in the atmosphere, trapping more longwave radiation and enhancing radiative forcing at the top of atmosphere (Held and Soden 2000, Soden and Held 2006). Changes in the vertical lapse rate along with warming and increased tropical water vapor transport into the upper troposphere, releasing latent heat and causing greater upper atmospheric warming (Sherwood *et al* 2010). The warming intensifies the emission of longwave radiation to space, leading to a negative lapse rate feedback in the tropics (Colman 2001, Bony *et al* 2006), moderating global temperature changes under climate forcing. Despite some offsetting effects, the net feedback remains positive (Colman 2001, Bony *et al* 2006, Soden and Held 2006), resulting in greater warming signals at higher levels than at lower levels.

3.3. Zonal mean temperature TOE

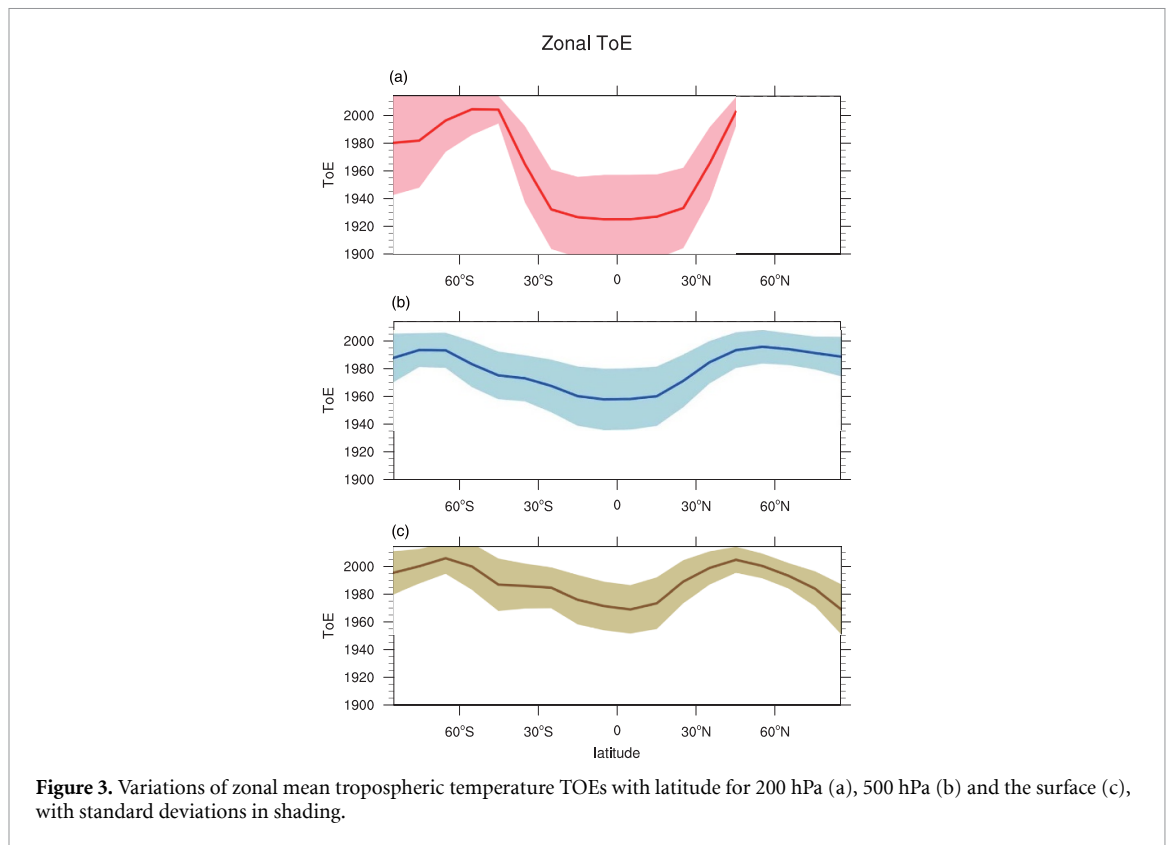
Given that TOE of different-altitude tropospheric temperatures shows a certain latitudinal dependency, we presented the zonal mean temperature TOE



variations with latitude for each 10-degree interval (figure 3). The MEM TOEs at different levels reveal that the earliest TOE occurs in the tropics, where temperature signals emerge around the 1930–1980s, consistently followed by higher latitudes in the 1990 s, and the latest in mid-latitudes in the 2000s. The TOE latitude variation of 500 hPa and surface air temperature approximately displays an ‘M-type’ pattern from the South Pole to the North. Sequentially, TOE emerges in the tropics, high-latitudes, and mid-latitudes. Also, there are differences between models lead to some uncertainties in the altitude-dependency TOE in the tropics. For instance, the TOE range for surface air temperature in the tropics falls in 1980 ± 15 , while it occurs in 1965 ± 20 for 500 hPa temperature and 1930 ± 30 for 200 hPa temperature. Unlike the tropics, mid-to-high latitudes do not show the altitude-dependency TOE in tropospheric temperatures.

3.4. TOEs in regions with significant temperature changes in tropical oceans

As mentioned above, both observational evidence and model simulations indicate that the annual mean SST signals reflecting tropical warming emerge earlier in most equatorial Pacific regions, with the latest TOE occurring in the eastern Pacific, which is also noted by Ying *et al* (2022). To further investigate the contrasting features in the equatorial Pacific, we selected the western equatorial Pacific (WEP) (0° – 16° N, 125° – 165° E) and the eastern equatorial Pacific (EEP) (10° S– 10° N, 180° W– 100° W) as two representative regions (figure 2(o)) and showed the regional mean MEM signal and noise sequences of the temperature change at different levels (figure 4). When the signal and noise curves intersect and the former is always greater than latter, the year corresponding to the intersection point is designated as the regional TOE. Consistent with tropospheric temperature TOEs in



the tropics, WEP and EEP show that 200 hPa temperature TOE is the earliest (1920–30s, figures 4(a) and (b)), surface air temperature is the latest (1960–90s, figures 4(e) and (f)), and 500 hPa temperature occurs between the two (1950–70s, figures 4(c) and (d)). The TOEs in WEP are generally 10–30 years earlier than those in EEP due to its greater noise. The robustness and uncertainty of the regional MEM TOE are in supplementary information part III.

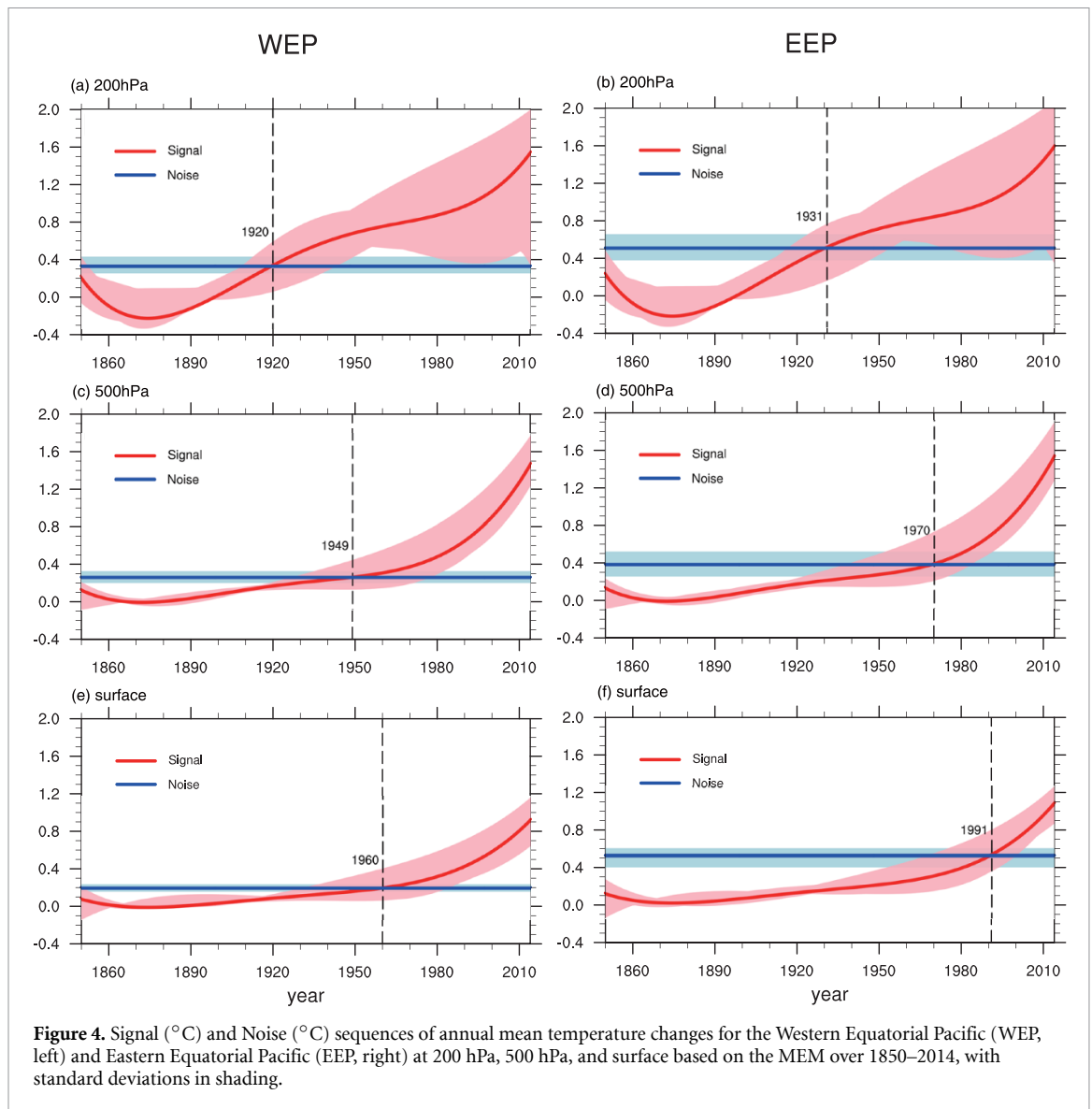
3.5. Surface air temperature TOEs in three major economies of the world

China, the European Union including 27 countries (EU27) and the United States (US) (figure 5(a)), as the three largest economies in the world, contributed to major global carbon emissions (Friedlingstein *et al* 2022, United Nations Statistics Division 2022). These three regions exhibited significant differences in the start timing of massive local carbon emissions. Since the early 19th century, the U.S. and the EU27 were significant contributors to CO₂ emissions (figures 5(b) and (c)). The emissions of the EU27 peaked in the 1860s, maintaining until the late 19th century, before declining. In contrast, the U.S. peaked in the 1940s. Subsequently, China was a noteworthy contributor to CO₂ emissions (figure 5(d)), with this upward trajectory persisting (Ritchie *et al* 2020). However, as shown in figures 5(e)–(g), the surface air temperature TOE in three economies showed consistency in the TOEs (the early 21st century). Notably, the U.S. and the EU27 exhibited strong

warming but larger noise compared to China, resulting in similar TOEs (figures 5(e)–(g)). Analysis of the Detection and Attribution Model Intercomparison Project (DAMIP) single greenhouse gases (GHG) forcing only experiments (Gillett *et al* 2016) revealed earlier TOE over globe than all forcing-induced TOE (supplementary information part V). Three economic regions showed 20–30 year earlier TOE in GHG only experiment in comparison with those estimated in CMIP6 historical experiments. The latter TOEs in historical simulations than those in GHG only simulations are due to the fact that GHG induced warming are partially offset by the local aerosol induced cooling (Duan *et al* 2019). Regions at the same latitude demonstrated a consistent TOE of surface air temperatures, irrespective of variations in the initiation and peak timing of regional carbon emissions.

3.6. Surface air temperature TOE in land and ocean at various latitudes in the Northern and Southern Hemispheres

Divergences in the TOEs are evident both between ocean and land at the same latitudes and across the various latitudes within the Northern (NH) and Southern (SH) Hemispheres. For the differences between ocean and land, the land–ocean warming contrast driven by more rapid surface air temperature increase over land than the ocean (Joshi *et al* 2008, Dong *et al* 2009), results in earlier TOE in land at all latitudes except for the ocean at high latitudes



in the NH. It is related to amplified Arctic warming (England *et al* 2021, Rantanen *et al* 2022), resulting in a larger signal in the NH high-latitude ocean (figures 6(a) and (b)). The SH high-latitude land and ocean (figures 6(c) and (d)) show similar signals, but TOEs are later over the ocean due to greater noise. The mid- and low-latitude lands in the NH and SH experience larger warming and relative larger noise, leading to earlier TOE. For the north–south differences across the various latitudes within the two hemispheres, the signal, noise and TOE in the low latitudes (figures 6(i)–(l)) are relatively similar, while the TOE in the SH middle latitudes (figures 6(g) and (h)) is earlier than that in the NH (figures 6(e) and

(f)) due to lower noise in the former. Additionally, the signal in the NH high latitudes is significantly greater than that in the SH (figures 2(f) and 6(a)–(d)), resulting in an earlier TOE in the NH high latitudes. To assess the robustness of regional TOEs over different latitude bands over land and ocean, we estimated years of TOEs in those regions for each model (results not shown). All models indicate an earlier TOE over ocean than over land for the NH high-latitude. In other latitude band regions, only one model gives opposite TOE contrast between land and ocean in comparison with those in other models and MEM. These results indicate robust estimation of land–ocean contrast among different models.

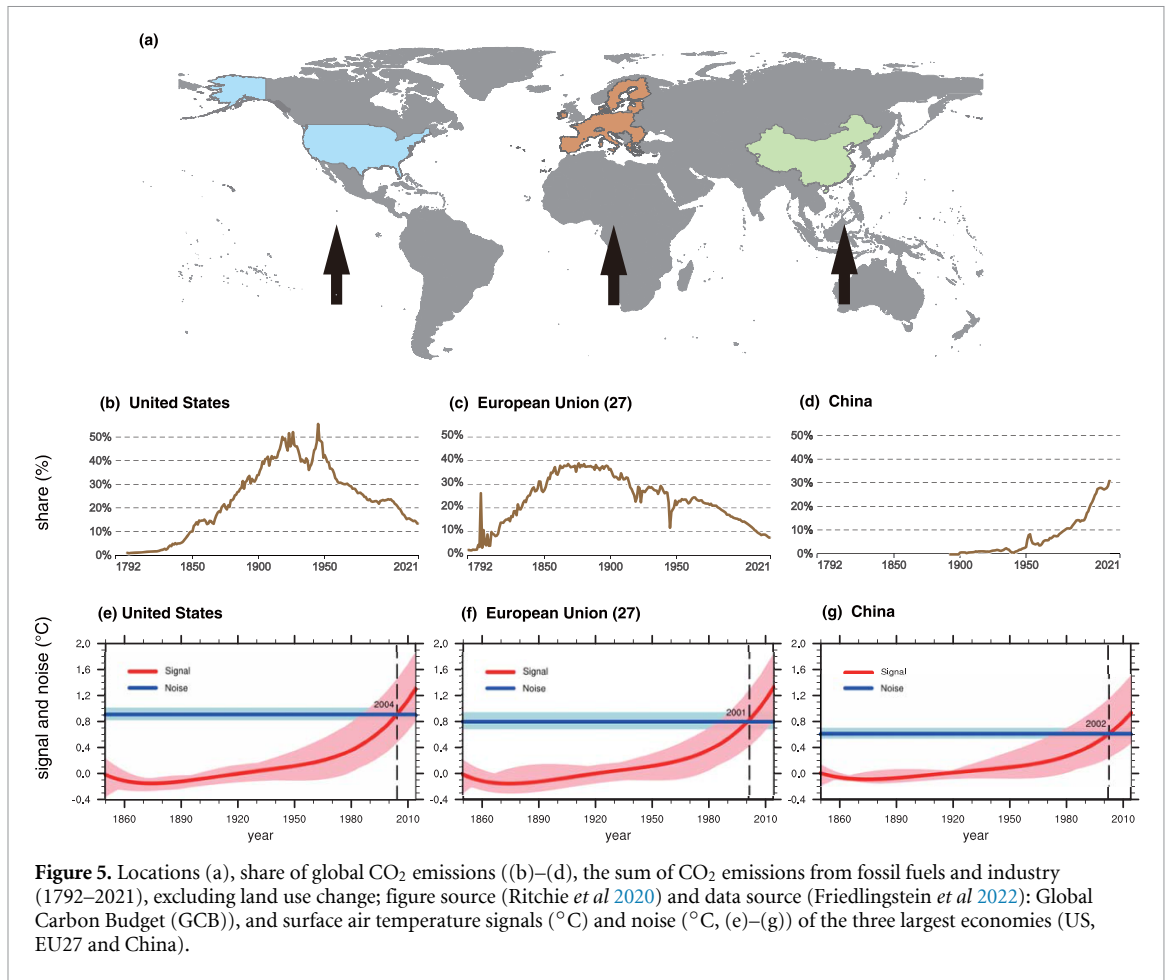


Figure 5. Locations (a), share of global CO₂ emissions ((b)–(d)), the sum of CO₂ emissions from fossil fuels and industry (1792–2021), excluding land use change; figure source (Ritchie *et al* 2020) and data source (Friedlingstein *et al* 2022): Global Carbon Budget (GCB), and surface air temperature signals (°C) and noise (°C, (e)–(g)) of the three largest economies (US, EU27 and China).

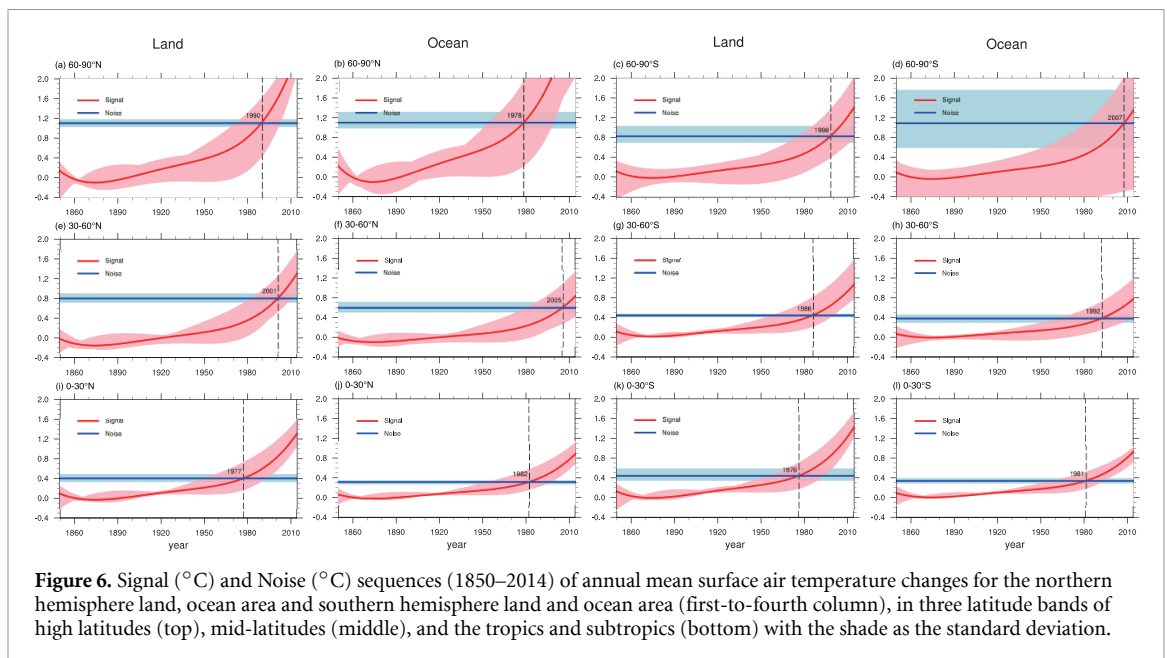


Figure 6. Signal (°C) and Noise (°C) sequences (1850–2014) of annual mean surface air temperature changes for the northern hemisphere land, ocean area and southern hemisphere land and ocean area (first-to-fourth column), in three latitude bands of high latitudes (top), mid-latitudes (middle), and the tropics and subtropics (bottom) with the shade as the standard deviation.

4. Conclusion and discussion

Based on the CMIP6 multi-model simulated air temperatures since the industrial revolution, we defined

the TOE as the first year in which the SNR consistently exceeds the threshold value of 1. We systematically analyzed the spatiotemporal characteristics of the TOE for temperature changes, especially differences

in different levels in the troposphere and over different regions. The main conclusions are summarized as follows:

- (1) Zonal means demonstrate the earliest TOEs for temperatures at different levels occur in the tropics, the latest in the mid-latitudes, and the variations in TOE from Antarctica to the Arctic exhibit an ‘M-type’ pattern, especially in the lower and middle troposphere.
- (2) Subject to the feedback effects of the temperature lapse rate change and deep convection changes in response to anthropogenic forcings, the signal in the tropical troposphere generally increases with altitude, the TOE becomes earlier there. Both the eastern and western equatorial Pacific regional TOEs emerge the earliest (1920–30s) for upper tropospheric temperature, followed by mid-tropospheric temperature (1950–70s), latest for surface air temperature (1960–90s). Western equatorial Pacific regional TOE is earlier, probably due to the larger internal climate variability in the eastern equatorial Pacific region influenced by ENSO.
- (3) For surface air temperature TOEs, there are some similarities in different countries and differences between oceans and lands at various latitudes. The three regions with large economy and carbon emissions—the EU27, the U.S. and China exhibit similar TOEs mainly due to that GHG induced warming are partially offset by the local aerosol induced cooling. The differences in TOE across ocean and land at the same latitudes, as well as between the two hemispheres at various latitudes, are influenced by anthropogenic forcings and regional climate dynamics. Aside from the high-latitude oceans in the NH where the surface air temperature TOE precedes that of lands, the TOE of lands at other latitudes consistently precedes that of oceans. In the low latitudes, both land and ocean exhibit relatively similar signal, noise, and TOE. In the mid-latitudes, TOE occurs earlier in the SH, attributed to lower noise. In contrast, the NH high latitudes display significantly greater signal intensity compared to SH, resulting in an earlier TOE.

The tropospheric temperature TOE in the tropics was the earliest compared to mid- and high-latitudes and became earlier with increasing altitude in the troposphere. Inconsistent with the decrease in SNR with increasing of the latitude (Hansen *et al* 1988), TOE follows an ‘M-type’ distribution with latitude between the South and North Poles. Differing from recent study (Santer *et al* 2019) reporting a close detection time in the lower and mid-to-high troposphere, we propose that in the tropics, the TOE of temperature advances with increasing altitude. The

vertical profile of temperature change is an important fingerprint of climate change (Santer *et al* 2013). The earlier emergence of the TOE in the upper tropospheric temperatures may serve as an early warning signal and is of great significance in the context of global warming. Accurately estimating the tropospheric temperature TOEs in the tropics helps to understand the sensitivity of the tropical climate system to anthropogenic forcing. It is also crucial for studying climate feedback mechanisms like water vapor (Minschwaner and Dessler 2004), lapse rate (Keil *et al* 2021) and cloud (Saint-Lu *et al* 2020) feedbacks, which can either amplify or dampen the warming effect and are vital in projecting future climate. Changes in tropical tropospheric temperatures and associated meridional temperature gradient affect weather patterns far beyond the tropics, e.g. the pronounced warming in the tropical upper troposphere may drive the poleward shift of the jet streams (Lorenz and DeWeaver 2007, Archer and Caldeira 2008, Rivière 2011, Woollings *et al* 2023). Previous research also indicated that storm tracks typically migrate poleward with rising radiative equilibrium temperature and increased tropical convective stability (Mbengue and Schneider 2013).

There are notable regional TOE differences in the tropics. The east and west equatorial Pacific exhibit a ‘seesaw’ pattern in SST and thermocline depth, which is characteristic of the strongest ocean-atmosphere coupling process known as El Niño–Southern Oscillation (ENSO) (Tsonis *et al* 2003, McPhaden *et al* 2006, Wang 2018). We revealed difference between two regional tropospheric temperature TOE. Specifically, the TOE occurs 10–30 years earlier in the warm pool than that in the cold tongue. The possible causes of this phenomenon are as follows: Weller *et al* (2016) and Bai *et al* (2022) detected the influence of human activities in the rapid warming and expansion in the Indo-Pacific Warm Pool (IPWP) using the optimal fingerprinting method. During the warming process of the warm pool, SST anomalies have been shown to impact the ENSO cycle (Wang *et al* 1999). Previous studies showed that the formation of ENSO is closely related to the anomalous thermal state of the western Pacific warm pool (Clarke *et al* 2000, Solomon and Jin 2005), especially to the eastward expansion of the warm water in the warm pool (McPhaden and Picaut 1990). The frequency of central Pacific El Niño events (Kao and Yu 2009, Kug *et al* 2009, Lee and McPhaden 2010, Freund *et al* 2019) as well as extreme La Niña occurrences have gradually increased in recent decades (Cai *et al* 2015, Dieppois *et al* 2021). Reconstructions of paleo-ENSO also indicated that ENSO activity was significantly stronger in the twentieth century than in previous centuries (Li *et al* 2013, McGregor *et al* 2013). The EEP have shown higher interannual variability than WEP (Wang *et al* 2017, Hawkins *et al* 2020). Consequently, there are regional differences

in the internal climate variability across the equatorial Pacific, with a delayed emergence in the eastern equatorial Pacific compared to the western.

Data availability statement

The data that support the findings of this study are openly available at the following URL/DOI: the CMIP6 data (<https://esgf-node.llnl.gov/search/cmip6/>), the ERA5 reanalysis data (www.ecmwf.int/en/forecasts/datasets/reanalysis-datasets/era5) and the ERSSTv5 (NOAA) data (<https://climatedataguide.ucar.edu/climate-data/sst-data-noaa-extended-reconstruction-ssts-version-5-ersstv5>).

Acknowledgments


This study was supported by the National Natural Science Foundation of China (41991254), the Strategic Priority Research Program of the Chinese Academy of Sciences (XDB40030100), and the Fund of Shandong Province (LSKJ202203300). We acknowledge the World Climate Research Programme's Working Group on Coupled Modelling, which is responsible for CMIP, and the climate modelling groups for producing and making available their model output.

Conflict of interest

The authors declare no competing interests.

ORCID iDs

Xiaodong Liu  <https://orcid.org/0000-0003-0355-5610>

Buwen Dong  <https://orcid.org/0000-0003-0809-7911>

References

- Allen M R *et al* 2018 Framing and Context *Global Warming of 1.5 °C. An IPCC Special Report on the Impacts of Global Warming of 1.5 °C Above Pre-Industrial Levels and Related Global Greenhouse Gas Emission Pathways, in the Context of Strengthening the Global Response to the Threat of Climate Change, Sustainable Development, and Efforts to Eradicate Poverty* (Cambridge University Press) pp 49–92
- Archer C L and Caldeira K 2008 Historical trends in the jet streams *Geophys. Res. Lett.* **35** 8
- Bai W R, Liu H L, Lin P F, Hu S J and Wang F 2022 Indo-Pacific warm pool present warming attribution and future projection constraint *Environ. Res. Lett.* **17** 054026
- Bindoff N L *et al* 2013 Detection and attribution of climate change: from global to regional *Climate Change 2013: the Physical Science Basis* (Cambridge University Press) pp 867–952 (<https://doi.org/10.1017/CBO9781107415324.022>)
- Bony S *et al* 2006 How well do we understand and evaluate climate change feedback processes? *J. Clim.* **19** 3445–82
- Cai W J *et al* 2015 Increased frequency of extreme La Nina events under greenhouse warming *Nat. Clim. Change* **5** 132–7
- Chen J, Li X Q, Martel J L, Brissette F P, Zhang X C J and Frei A 2021 Relative importance of internal climate variability versus anthropogenic climate change in global climate change *J. Clim.* **34** 465–78
- Chen X Y and Tung K K 2018 Global-mean surface air temperature variability: space-time perspective from rotated EOFs *Clim. Dyn.* **51** 1719–32
- Christensen J H *et al* 2007 Regional climate projections *Climate Change 2007: the Physical Science Basis. Contribution of Working Group I to the Fourth Assessment Report of the Intergovernmental Panel on Climate Change* (Cambridge University Press) pp 847–940
- Clarke A J, Wang J G and Van Gorder S 2000 A simple warm-pool displacement ENSO model *J. Phys. Oceanogr.* **30** 1679–91
- Colman R A 2001 On the vertical extent of atmospheric feedbacks *Clim. Dyn.* **17** 391–405
- Connors S *et al* 2022 *Climate Change 2021: Summary for All* (Intergovernmental Panel on Climate Change) p 4
- Dai A G, Fyfe J C, Xie S P and Dai X G 2015 Decadal modulation of global surface air temperature by internal climate variability *Nat. Clim. Change* **5** 555
- Deser C, Knutti R, Solomon S and Phillips A S 2012a Communication of the role of natural variability in future North American climate *Nat. Clim. Change* **2** 775–9
- Deser C, Phillips A, Bourdette V and Teng H Y 2012b Uncertainty in climate change projections: the role of internal variability *Clim. Dyn.* **38** 527–46
- Deser C, Terray L and Phillips A S 2016 Forced and internal components of winter air temperature trends over North America during the past 50 years: mechanisms and implications *J. Clim.* **29** 2237–58
- Dieppois B, Capotondi A, Pohl B, Chun K P, Monerie P A and Eden J 2021 ENSO diversity shows robust decadal variations that must be captured for accurate future projections *Commun. Earth Environ.* **2** 2122019
- Dong B W, Gregory J M and Sutton R T 2009 Understanding land-sea warming contrast in response to increasing greenhouse gases. Part I: transient adjustment *J. Clim.* **22** 3079–97
- Dong L and McPhaden M J 2017 The role of external forcing and internal variability in regulating global mean surface air temperatures on decadal timescales *Environ. Res. Lett.* **12** 034011
- Duan J *et al* 2019 Detection of human influences on temperature seasonality from the nineteenth century *Nat. Sustain.* **2** 484–90
- England M H, McGregor S, Spence P, Meehl G A, Timmermann A, Cai W, Gupta A S, McPhaden M J, Purich A and Santoso A 2014 Recent intensification of wind-driven circulation in the Pacific and the ongoing warming hiatus *Nat. Clim. Change* **4** 222–7
- England M R, Eisenman I, Lutsko N J and Wagner T J W 2021 The recent emergence of Arctic amplification *Geophys. Res. Lett.* **48** e2021GL094086
- Estrada F, Kim D and Perron P 2021 Anthropogenic influence in observed regional warming trends and the implied social time of emergence *Commun. Earth Environ.* **2** 31
- Eyring V *et al* 2021 Human influence on the climate system *Climate Change 2021: the Physical Science Basis. Contribution of Working Group I to the Sixth Assessment Report of the Intergovernmental Panel on Climate Change* (Cambridge University Press) pp 423–552
- Eyring V, Bony S, Meehl G A, Senior C A, Stevens B, Stouffer R J and Taylor K E 2016 Overview of the Coupled Model Intercomparison Project Phase 6 (CMIP6) experimental design and organization *Geosci. Model. Dev.* **9** 1937–58
- Fischer E M and Knutti R 2014 Detection of spatially aggregated changes in temperature and precipitation extremes *Geophys. Res. Lett.* **41** 547–54
- Freund M B, Henley B J, Karoly D J, McGregor H V, Abram N J and Dommenget D 2019 Higher frequency of Central Pacific El Niño events in recent decades relative to past centuries *Nat. Geosci.* **12** 450
- Friedlingstein P *et al* 2022 Global carbon budget 2022 vol 2022 pp 1–159

- Fu Q, Johanson C M, Warren S G and Seidel D J 2004 Contribution of stratospheric cooling to satellite-inferred tropospheric temperature trends *Nature* **429** 55–58
- Fu Q, Manabe S and Johanson C M 2011 On the warming in the tropical upper troposphere: models versus observations *Geophys. Res. Lett.* **38** L15704
- Gillett N P, Shiogama H, Funke B, Hegerl G, Knutti R, Matthes K, Santer B D, Stone D and Tebaldi C 2016 The detection and attribution model intercomparison project (DAMIP v1.0) contribution to CMIP6 *Geosci. Model Dev.* **9** 3685–97
- Gillett P et al 2021 Constraining human contributions to observed warming since the pre-industrial period *Nat. Clim. Change* **11** 207–12
- Giorgi F and Bi X Q 2009 Time of emergence (TOE) of GHG-forced precipitation change hot-spots *Geophys. Res. Lett.* **36** L06709
- Hansen J, Fung I, Lacis A, Rind D, Lebedeff S, Ruedy R, Russell G and Stone P 1988 Global climate changes as forecast by goddard institute for space studies 3-dimensional model *J. Geophys. Res. Atmos.* **93** 9341–64
- Haustein K, Allen M R, Forster P M, Otto F E L, Mitchell D M, Matthews H D and Frame D J 2017 A real-time Global Warming Index *Sci. Rep.* **7** 15417
- Hawkins E, Frame D, Harrington L, Joshi M, King A, Rojas M and Sutton R 2020 Observed emergence of the climate change signal: from the familiar to the unknown *Geophys. Res. Lett.* **47** e2019GL086259
- Hawkins E and Sutton R 2009 The potential to narrow uncertainty in regional climate predictions *Bull. Am. Meteorol. Soc.* **90** 1095
- Hawkins E and Sutton R 2012 Time of emergence of climate signals *Geophys. Res. Lett.* **39** L01702
- Held I M and Soden B J 2000 Water vapor feedback and global warming *Annu. Rev. Environ. Resour.* **25** 441–75
- Hersbach H et al 2020 The ERA5 global reanalysis *Q. J. R. Meteorol. Soc.* **146** 1999–2049
- Huang B Y, Thorne P W, Banzon V F, Boyer T, Chepurin G, Lawrimore J H, Menne M J, Smith T M, Vose R S and Zhang H-M 2017 Extended reconstructed sea surface air temperature, version 5 (ERSSTv5): upgrades, validations, and intercomparisons *J. Clim.* **30** 8179–205
- Hulme M, Barrow E M, Arnell N W, Harrison P A, Johns T C and Downing T E 1999 Relative impacts of human-induced climate change and natural climate variability *Nature* **397** 688–91
- Im E S et al 2021 Emergence of robust anthropogenic increase of heat stress-related variables projected from CORDEX-CORE climate simulations *Clim. Dyn.* **57** 1629–44
- Jones P D, New M, Parker D E, Martin S and Rigor I G 1999 Surface air temperature and its changes over the past 150 years *Rev. Geophys.* **37** 173–99
- Joshi M M, Gregory J M, Webb M J, Sexton D M H and Johns T C 2008 Mechanisms for the land/sea warming contrast exhibited by simulations of climate change *Clim. Dyn.* **30** 455–65
- Kao H Y and Yu J Y 2009 Contrasting Eastern-Pacific and Central-Pacific types of ENSO *J. Clim.* **22** 615–32
- Karoly D J and Wu Q G 2005 Detection of regional surface air temperature trends *J. Clim.* **18** 4337–43
- Keil P, Schmidt H, Stevens B and Bao J 2021 Variations of tropical lapse rates in climate models and their implications for upper-tropospheric warming *J. Clim.* **34** 9747–61
- King A D, Donat M G, Fischer E M, Hawkins E, Alexander L V, Karoly D J, Dittus A J, Lewis S C and Perkins S E 2015 The timing of anthropogenic emergence in simulated climate extremes *Environ. Res. Lett.* **10** 094015
- Kosaka Y and Xie S P 2016 The tropical Pacific as a key pacemaker of the variable rates of global warming *Nat. Geosci.* **9** 669
- Kug J S, Jin F F and An S I 2009 Two types of El Niño events: cold tongue El Niño and warm pool El Niño *J. Clim.* **22** 1499–515
- Lee T and McPhaden M J 2010 Increasing intensity of El Niño in the central-equatorial Pacific *Geophys. Res. Lett.* **37** L14603
- Lehner F, Deser C and Terray L 2017 Toward a new estimate of ‘time of emergence’ of anthropogenic warming: insights from dynamical adjustment and a large initial-condition model ensemble *J. Clim.* **30** 7739–56
- Li J B et al 2013 El Niño modulations over the past seven centuries *Nat. Clim. Change* **3** 822–6
- Liu X D and Chen B D 2000 Climatic warming in the Tibetan Plateau during recent decades *Int. J. Climatol.* **20** 1729–42
- Lorenz D J and DeWeaver E T 2007 Tropopause height and zonal wind response to global warming in the IPCC scenario integrations *J. Geophys. Res. Atmos.* **112** D10
- Mahlstein I, Hegerl G and Solomon S 2012 Emerging local warming signals in observational data *Geophys. Res. Lett.* **39** L21711
- Mahlstein I, Knutti R, Solomon S and Portmann R W 2011 Early onset of significant local warming in low latitude countries *Environ. Res. Lett.* **6** 034009
- Manabe S and Wetherald R T 1967 Thermal equilibrium of atmosphere with a given distribution of relative humidity *J. Atmos. Sci.* **24** 241–59
- Manabe S and Wetherald R T 1975 Effects of doubling CO₂ concentration on climate of a general circulation model *J. Atmos. Sci.* **32** 3–15
- Mbengue C and Schneider T 2013 Storm track shifts under climate change: what can be learned from large-scale dry dynamics *J. Clim.* **26** 9923–30
- McGregor S, Timmermann A, England M H, Timm O E and Wittenberg A T 2013 Inferred changes in El Niño-Southern Oscillation variance over the past six centuries *Clim. Past* **9** 2269–84
- McPhaden M J and Picaut J 1990 El-niño southern oscillation displacements of the western equatorial Pacific warm pool *Science* **250** 1385–8
- McPhaden M J, Zebiak S E and Glantz M H 2006 ENSO as an integrating concept in Earth science *Science* **314** 1740–5
- Medhaug I, Stolpe M B, Fischer E M and Knutti R 2017 Reconciling controversies about the ‘global warming hiatus’ *Nature* **545** 41
- Meehl G A, Hu A X, Santer B D and Xie S P 2016 Contribution of the Interdecadal Pacific Oscillation to twentieth-century global surface air temperature trends *Nat. Clim. Change* **6** 1005–8
- Minschwaner K and Dessler A E 2004 Water vapor feedback in the tropical upper troposphere: model results and observations *J. Clim.* **17** 1272–82
- Mitchell D M, Thorne P W, Stott P A and Gray L J 2013 Revisiting the controversial issue of tropical tropospheric temperature trends *Geophys. Res. Lett.* **40** 2801–6
- Pepin N et al 2015 Elevation-dependent warming in mountain regions of the world *Nat. Clim. Change* **5** 424–30
- Po-Chedley S, Armour K C, Bitz C M, Zelinka M D, Santer B D and Fu Q 2018 Sources of intermodel spread in the lapse rate and water vapor feedbacks *J. Clim.* **31** 3187–206
- Rantanen M, Karpechko A Y, Lipponen A, Nordling K, Hyvärinen O, Ruosteenoja K, Vihma T and Laaksonen A 2022 The Arctic has warmed nearly four times faster than the globe since 1979 *Commun. Earth Environ.* **3** 168
- Ritchie H, Roser M and Rosado P 2020 CO₂ and greenhouse gas emissions (Our.World.In.Data) (available at: <https://ourworldindata.org/co2-and-greenhouse-gas-emissions>)
- Rivière G 2011 A dynamical interpretation of the poleward shift of the jet streams in global warming scenarios *J. Atmos. Sci.* **68** 1253–72
- Saint-Lu M, Bony S and Dufresne J L 2020 Observational evidence for a stability Iris effect in the tropics *Geophys. Res. Lett.* **47** 14
- Santer B D et al 2005 Amplification of surface air temperature trends and variability in the tropical atmosphere *Science* **309** 1551–6
- Santer B D et al 2013 Identifying human influences on atmospheric temperature *Proc. Natl Acad. Sci. USA* **110** 26–33

- Santer B D *et al* 2017 Comparing tropospheric warming in climate models and satellite data *J. Clim.* **30** 373–92
- Santer B D, Fyfe J C, Solomon S, Painter J F, Bonfils C and Pallotta G 2019 Quantifying stochastic uncertainty in detection time of human-caused climate signals *Proc. Natl Acad. Sci. USA* **116** 19821–7
- Sherwood S C, Roca R, Weckwerth T M and Andronova N G 2010 Tropospheric water vapor, convection, and climate *Rev. Geophys.* **48** RG2001
- Soden B J and Held I M 2006 An assessment of climate feedbacks in coupled ocean-atmosphere models *J. Clim.* **19** 3354–60
- Solomon A and Jin F F 2005 A study of the impact of off-equatorial warm pool SST anomalies on ENSO cycles *J. Clim.* **18** 274–86
- Solomon S *et al* 2007 *Climate Change 2007: the Physical Science Basis: Working Group I Contribution to the Fourth Assessment Report of the IPCC* (Cambridge University Press)
- Steinman B A, Mann M E and Miller S K 2015 Atlantic and Pacific multidecadal oscillations and Northern Hemisphere temperatures *Science* **347** 988–91
- Stocker T *et al* 2014 *Climate Change 2013: the Physical Science Basis: Working Group I Contribution to the Fifth Assessment Report of the Intergovernmental Panel on Climate Change* (Cambridge University Press) (<https://doi.org/10.1017/CBO9781107415324>)
- Stott P A, Tett S F B, Jones G S, Allen M R, Mitchell J F B and Jenkins G J 2000 External control of 20th century temperature by natural and anthropogenic forcings *Science* **290** 2133–7
- Taylor K E 2001 Summarizing multiple aspects of model performance in a single diagram *J. Geophys. Res. Atmos.* **106** 7183–92
- Tebaldi C and Knutti R 2007 The use of the multi-model ensemble in probabilistic climate projections *Phil. Trans. R. Soc. A* **365** 2053–75
- Tett S F B, Stott P A, Allen M R, Ingram W J and Mitchell J F B 1999 Causes of twentieth-century temperature change near the Earth's surface *Nature* **399** 569–72
- Tsonis A A, Hunt A G and Elsner J B 2003 On the relation between ENSO and global climate change *Meteorol. Atmos. Phys.* **84** 229–42
- United Nations Statistics Division 2022 National accounts main aggregates database (available at: <https://unstats.un.org/unsd/snaama/dnllist.asp>) (Accessed 1 January 2022)
- Vallis G K, Zurita-Gotor P, Cairns C and Kidston J 2015 Response of the large-scale structure of the atmosphere to global warming *Q. J. R. Meteorol. Soc.* **141** 1479–501
- Wang B, Zheng L H, Liu D L, Ji F, Clark A and Yu Q 2018 Using multi-model ensembles of CMIP5 global climate models to reproduce observed monthly rainfall and temperature with machine learning methods in Australia *Int. J. Climatol.* **38** 4891–902
- Wang C Y, Xie S P, Kosaka Y, Liu Q Y and Zheng X T 2017 Global influence of tropical Pacific variability with implications for global warming slowdown *J. Clim.* **30** 2679–95
- Wang C Z 2018 A review of ENSO theories *Natl Sci. Rev.* **5** 813–25
- Wang C Z, Weisberg R H and Virmani J I 1999 Western Pacific interannual variability associated with the El Niño Southern Oscillation *J. Geophys. Res. Oceans* **104** 5131–49
- Wei M, Qiao F L, Guo Y Q, Deng J, Song Z Y, Shu Q and Yang X D 2019 Quantifying the importance of interannual, interdecadal and multidecadal climate natural variabilities in the modulation of global warming rates *Clim. Dyn.* **53** 6715–27
- Weller E, Min S K, Cai W J, Zwiers F W, Kim Y H and Lee D 2016 Human-caused Indo-Pacific warm pool expansion *Sci. Adv.* **2** e1501719
- Woollings T, Drouard M, O'Reilly C H, Sexton D M H and McSweeney C 2023 Trends in the atmospheric jet streams are emerging in observations and could be linked to tropical warming *Commun. Earth Environ.* **4** 125
- Ying J, Collins M, Cai W J, Timmermann A, Huang P, Chen D K and Stein K 2022 Emergence of climate change in the tropical Pacific *Nat. Clim. Change* **12** 356
- Zhang H H and Delworth T L 2018 Robustness of anthropogenically forced decadal precipitation changes projected for the 21st century *Nat. Commun.* **9** 1150